Some Effects of Surface Heating and Topography on the Regional Severe Storm Environment. Part II: Two-Dimensional Idealized Experiments

STANLEY G. BENJAMIN

National Center for Atmospheric Research, Boulder, CO, and Program for Regional Observing and Forecasting Systems, NOAA, Environmental Research Laboratories, Boulder, CO 80303*

(Manuscript received 3 July 1984, in final form 3 August 1985)

ABSTRACT

A series of two-dimensional (2-D) numerical experiments has been conducted to examine the effects of differential surface heating on flow over a dry, 2000 km-wide plateau. Two effects, found by Benjamin and Carlson in three-dimensional simulations to be significant in the regional severe storm environment, also occur in these 2-D experiments. These effects are a diurnal variation in the intensity of the lee trough and the development of a low-level inversion downstream as the mixed layer, which developed over the hot plateau, is advected over potentially cooler air.

When the plateau is strongly heated and surrounded by lowlands with no surface heating, the leeside pressure trough intensifies by an extra 1–3 mb. Subsequently, the low-level flow ahead of the lee trough also increases by several meters per second when surface heating is allowed. The diurnal modulation of this feature suggests that the low-level moist flow toward regions of potential convection in cases such as those modeled by Benjamin and Carlson will tend to be strongest in the late afternoon and early evening. It is shown that this effect is primarily due to the superposition of a plateau heat low upon the mountain wave circulation. To a lesser extent, differential vertical mixing of momentum between the deep mixed layer and surrounding regions also tends to enhance the lee trough. This differential mixing momentum mechanism is active in the presence of an isolated, deep mixed layer and moderately strong lower tropospheric flow even if there is no elevated terrain.

The development of the elevated mixed layer inversion appears to depend more strongly on a horizontal gradient of soil moisture and surface heating than it does upon a gradient of terrain elevation. However, while such an inversion may be produced by differential advection and differential heating in the absence of terrain, it will be stronger and develop more rapidly in a shearing environment if the strongly heated region is also elevated.

1. Introduction

Although a large number of studies have concerned various aspects of flow over mountains, a somewhat smaller number of these studies have treated the behavior of this flow in the presence of surface heating. However, a variety of atmospheric features have been specifically related to surface heating of elevated terrain, ranging in scale from mountain–valley breezes to monsoon circulations. In a companion paper, Benjamin and Carlson (1986, hereafter referred to as BC) have used three-dimensional simulations of south central United States severe storm cases to demonstrate how effects jointly produced by surface heating and topography may not only focus the region where severe convective storms are most likely to occur but even enhance their intensity. These effects are further investigated in a series of idealized two-dimensional (2-D) experiments which are described in this paper.

Although the capping inversion in the pre-severe storm environment has been commonly attributed to subsidence, Carlson and Ludlam (1968) and Carlson et al. (1980; 1983) have shown that this inversion may also be produced by advection of a hot mixed layer, formed over dry elevated terrain, downstream over moist, potentially cooler air. In different cases over Europe and North America illustrated in these articles, such elevated mixed layer restraining inversions typically exhibited a relatively sharp boundary at the streamline on their northern and western sides. The outbreak of severe convective storms is often located where low-level moist air flows under the northern boundary of the elevated mixed layer plume toward cooler air aloft. Thus, this type of inversion acts not only as a delay, preventing deep convection over a wide area while heat and moisture build up in the boundary layer, but also acts as a focusing feature.

Benjamin and Carlson showed the dependence upon surface heating of both the elevated mixed layer restraining inversion as well as a daytime intensification of the leeside pressure trough (and the low-level moist flow ahead of it) in simulations of both the SESAME I (10–11 April 1979) and SESAME IV (9–10 May 1979) cases. Their results suggested that destabilization via underrunning (differential advection) and therefore, the

* The National Center for Atmospheric Research is sponsored by the National Science Foundation.

likelihood of strong convective storms at the lid edge, was at a maximum during the afternoon and early evening hours, coinciding with the time of maximum destabilization from surface heating. Benjamin and Carlson concluded that these two combined effects of surface heating and topography (elevated mixed layer inversions and daytime enhancement of lee troughing) appear to act in unison to focus the timing and position of certain severe storm outbreaks.

Based on the above results, this study attempts to isolate the physical mechanisms producing these effects by examining them in idealized 2-D experiments. The results of the 2-D experiments not only were consistent with those of the three-dimensional study, but also contributed additional relevant insights. A review of related studies in Section 2 is followed by a description of the 2-D model in Section 3. The diurnal variation of the leeside pressure trough and the development of the elevated mixed layer as they occurred in 2-D experiments are both discussed in Section 4. Finally, a summary of the results is presented in Section 5.

2. Background

The wide range of meteorological phenomena associated with mountain waves has been summarized by several authors, including Alaka (1960), Smith (1979) and Barry (1981). Queney (1948) first showed that the response of the atmosphere to stably stratified flow over a mountain barrier depends critically upon U/L, where U is the cross-barrier wind magnitude and L is the mountain half-width. The leeside trough with geostrophic flow is limited to situations where the mountain half-width is such that the residence time of air parcels over sloping terrain (U/L) is of the order $1/f$, where f is the Coriolis acceleration. Modeling studies of such intermediate to synoptic scale lee troughs have been performed for cases over the Rockies and Alps (e.g., Egger, 1974; Bleck, 1977; Anthes and Keyser, 1979; Tibaldi et al., 1980). However, neither these studies nor model simulations of smaller-scale mountain waves such as Klemp and Lilly (1978) have attempted to study the effects of boundary-layer processes such as sensible heating and vertical mixing of momentum.

Alternately, other researchers have examined regional-scale, thermally induced topographic circulations without consideration of ambient flow. These circulations include the diurnal sloping terrain wind system, which has been suggested as an explanation for the low-level jet (e.g., Bleeker and André, 1951; Holton, 1967; Lettau and Lettau, 1978; Reiter and Tang, 1984), circulations induced by soil moisture contrasts over idealized terrain (Ookouchi et al., 1984), and the monsoon circulation. Observations of the summer and winter monsoons forced by surface heating and cooling over the Tibetan (Qinghai-Xizang) plateau have been summarized by Gao et al. (1981). Tang and Reiter (1984) have found many similarities between the Asian monsoon and seasonal circulations apparently forced by surface heating and cooling over the western United States and Mexican plateaus.

Among studies which have considered boundary layer effects on flow over mountains, Raymond (1972) used an analytic solution to determine that surface heating dampens the perturbation in the flow whereas cooling has the opposite effect. This result is consistent with theoretical results of Klemp and Lilly (1975) showing that the presence of a low-level stable layer is conducive to strong mountain wave development. Queney (1948) suggested that mixing should exert a slight damping influence on mountain wave perturbations. On the other hand, enhanced lee troughing has been linked with increased surface friction by Buzzi and Tibaldi (1977) and Han et al. (1982). However, neither of these studies considered the effects of vertical mixing of momentum on flow over a ridge or plateau. Two-dimensional simulations of flow over a mountain with and without a diurnal heating cycle were performed by Mahrer and Pielke (1975) using a model including a K-coefficient boundary-layer parameterization. They found, as did BC, that the leeside low-level wind maximum was weakest in the presence of a neutral or unstable boundary layer with strong vertical mixing of momentum.

In the current study, the effects of differential heating on flow over a large-scale plateau are considered. The differential heating is generated by the variation in soil moisture between the dry plateau and moist lowlands. Such a decrease of soil moisture with elevation is found over Mexico, particularly in the spring. Barry (1981) summarizes observations showing that mean precipitation decreases with elevation above a certain level in Mexico as well as other subtropical and equatorial regions (between 30°N and 30°S), notably east Africa and Asia. This variation is often strongest in the pre-monsoon season. For instance, Tang and Reiter (1984) show that mean monthly precipitation over the southwest United States and Mexican plateaus is very sparse from winter to spring, but by late May or June, the influx of moisture from the monsoon circulation typically has reached the elevation of the high plateau. From then through the summer, convective rainfall is much more common over the plateau (Mosiño Aleman and Garcia, 1974) and differential heating between the plateau and lowlands is diminished. Tang and Reiter also describe similar seasonal variations of precipitation over the Tibetan plateau. Since both this paper and BC consider certain influences on the severe storm environment brought about by both differential heating and topography, it is noteworthy that the time of strongest differential heating between the Mexican plateau and the region to its east coincides with the spring severe storm maximum in the south central United States.

3. The two-dimensional model

A two-dimensional analog of the 3-D mesoscale model described in BC was used in this study to test atmospheric response to differential heating in the presence of flow over a large-scale plateau. This 2-D model is described in detail in Anthes and Warner (1978). The multilevel boundary layer model and radiation parameterization described in section 2 of BC were also used with the 2-D simulations. A correction to eliminate diffusion of temperature along constant sigma surfaces in regions of sloping terrain was also included. Other basic parameters are listed in Table 1.

An artificial dissipation layer with increased horizontal diffusion near the top of the model domain was applied. Klemp and Lilly (1978) recommended use of such a damping scheme in order to accurately model the upward propagation of energy which may occur with stably stratified flow over mountains. The form of the dissipation layer used here is similar to that of Anthes and Warner (1978) with K_H increasing from 8.0×10^3 m^2 s^{-1} at $\sigma = 0.39$ up to $K_H = 8.0 \times 10^5$ m^2 s^{-1} at the top of the model domain ($\sigma = 0.0$). The maximum K_H was chosen to ensure numerical stability.

In the two 1979 SESAME cases studied by BC, the Mexican plateau was identified as the source region for the heated air which later became an elevated mixed layer over parts of Texas and Oklahoma. Also, the lee trough which formed in these cases was located east of the steep terrain gradient on the eastern side of the Mexican plateau. Therefore, the profiles of terrain and surface characteristics across the domain for the basic heated plateau case were chosen to resemble those of the Mexican plateau, except that the model plateau is about twice as wide (2000 km) as that of Mexico (800–1000 km). The extra width ensures that air will reside over the model plateau for more than one diurnal heating period in 36 h simulations. The height of the terrain with an idealized plateau was specified with the function

$$h'(J) = \frac{1500}{\pi^2}\left\{\left[\frac{\pi}{2} + \tan^{-1}\left(\frac{J - X_1}{A}\right)\right] \times \left[\frac{\pi}{2} + \tan^{-1}\left(\frac{X_2 - J}{A}\right)\right]\right\} \quad (1)$$

where 1500 m is the maximum height of the plateau, J is the horizontal grid point (between 1 and 63), X_1 and X_2 are the grid points of the centers of the plateau sides (usually set at 21 and 43), and A is the slope half-width (usually set at 0.3). To decrease the slope on either side of the plateau, the final terrain profile was defined as

$$h(J) = [h'(J) + h'(J + 1)]/2. \quad (2)$$

This set the effective half-width as 0.7 grid lengths (80 km). The terrain shape from this function is illustrated in 2-D cross-section figures (e.g., Fig. 4a). A similar function was used by Queney (1948) to determine analytical solutions for flow over a plateau-shaped mountain.

A look-up table (Table 1 from BC) was again used to specify surface characteristics as a function of the surface index which was set at 7 (arid land) over the plateau and 0 (no surface heating—ocean) on the plateau sides and at low elevations. A second complete set of experiments were conducted in which surface heating was also allowed on the sides of the plateau. Although these experiments pointed to the same conclusions reached from experiments without heating on plateau sides, they are not shown in this paper since the effect of heating on the lee trough was exaggerated by the replacement of cooler air by heated air through a greater depth on the plateau sides than over the plateau.

For the 2-D experiments, the land values of surface emissivity were set at 0.9 and those of roughness length were set at 2 cm. No moist physics (rainfall, latent heat release, cloud parameterization, surface evaporative flux) were included in the 2-D experiments since they did not influence the mountain wave across Mexico in the 3-D simulations of BC. A precipitable water amount, necessary for radiation calculations, was specified to vary from 2.7 cm over low terrain to 1.2 cm over the plateau.

TABLE 1. Parameters for 2-D experiments.

Horizontal grid length (Δs)	111.11 km
Time step (Δt)	180 s
Horizontal grid size	63 points
Moist physics	none
Latitude at all points	20°N
Longitude at center of domain	104.5°W
Initial time for all forecasts	1200 GMT 3 May
Pressure at top of domain	100 mb
Sigma levels	20

Level	σ
1	0.0
2	0.04
3	0.08
4	0.12
5	0.16
6	0.20
7	0.25
8	0.305
9	0.36
10	0.416
11	0.471
12	0.529
13	0.586
14	0.643
15	0.718
16	0.798
17	0.855
18	0.915
19	0.998
20	1.0

A single idealized thermodynamic sounding (from subjectively averaged subtropical soundings) was used to initialize all 2-D model experiments. This sounding (depicted in Fig. 1) features a low-level stable layer from 1000 mb to about 840 mb, a large layer of lower stability from 840 to 300 mb, and another layer of slightly higher stability from 300 to 100 mb.

Two different geostrophic wind profiles, also shown in Fig. 1, were used for different sets of experiments. The initial wind was specified as geostrophic. Experiments with the shear profile also used a nonzero north–south temperature gradient ($\partial T/\partial y \neq 0$) for thermal wind consistency. Thus, the v component which developed in the model simulations advected warmer or cooler air in the cross-plane direction. The variation of geostrophic shear with height implies that the thermal structure must change in the y direction if the cross section were used to generate a 3-D field (D. Keyser, personal communication, 1984). Experiments were also performed using a second wind profile with u_g constant at 10 m s^{-1}. Thus, no N–S temperature advection occurred in this set of experiments.

4. Effects of surface heating and topography

Several indications of a standing mountain wave to the lee of the Mexican plateau were found in the 3-D numerical simulations of the 10–11 April 1979 case described in the companion article (BC). Typical mountain wave structures of potential temperature and vertical and horizontal motion are shown in Fig. 27 of BC, and a strong leeside pressure trough also developed. Some of these features were also noted by Anthes et al. (1982), who presented observational evidence for the same mountain wave in this case.

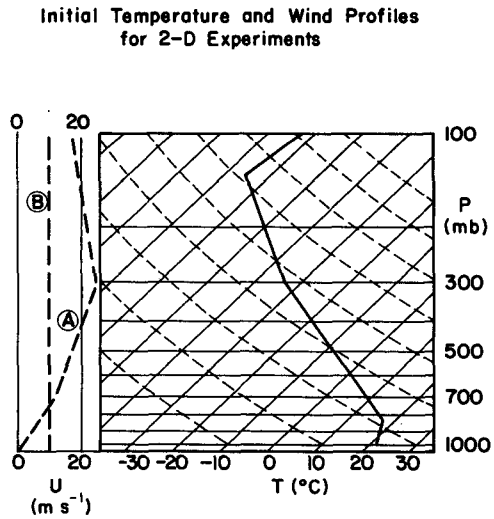

FIG. 1. Initial vertical profiles of temperature and wind (u) for 2-D model simulations. The geostrophic u component, u_g, is set equal to the initial u at all points; v and v_g are initially set equal to zero everywhere.

TABLE 2. Characteristics of 2-D experiments.

Experiment	U_g	Terrain	Surface heating over plateau	Duration
A-1	shear	plateau	N	36 h
A-1A	shear	plateau	N—no surface friction.	36 h
A-2	shear	plateau	Y	36 h
A-3	shear	flat	Y	36 h
A-4	shear	plateau	specified to be same as that in A-2; no vertical mixing of momentum.	12 h
A-5	shear	flat	specified to be same as that in A-3; no vertical mixing of momentum.	12 h
All of the above experiments were also carried out with the constant U_g profile and are denoted as Experiments B-1 through B-5.				
A-6	shear	plateau	Y—no N–S temperature advection.	36 h
A-7	shear	flat	Y—no N–S temperature advection.	36 h
A-8	shear	plateau	Y—heated allowed at all points rather than just over plateau.	12 h

A comparison between simulations with and without surface fluxes (BC and Anthes et al., 1982) suggested that vertical mixing of momentum could produce a decrease in low-level winds when surface fluxes were allowed. Moreover, 3-D sensitivity experiments from two separate cases from the 1979 SESAME field program (also described in BC) indicated that not only differential surface heating but also differential mixing of momentum may significantly intensify the leeside pressure trough. Mechanisms which may explain these effects are investigated in the 2-D experiments described in this section.

Three basic 36 h (day-night-day) experiments and a few additional 12 h experiments were conducted with each of the two wind profiles (Table 2). Most of these 2-D experiments included a plateau-shaped mountain in the middle of the domain.

a. Effects on surface pressure

The development of surface pressure features is first considered. The horizontal profile of surface pressure perturbation (change from initial conditions) at 12 h

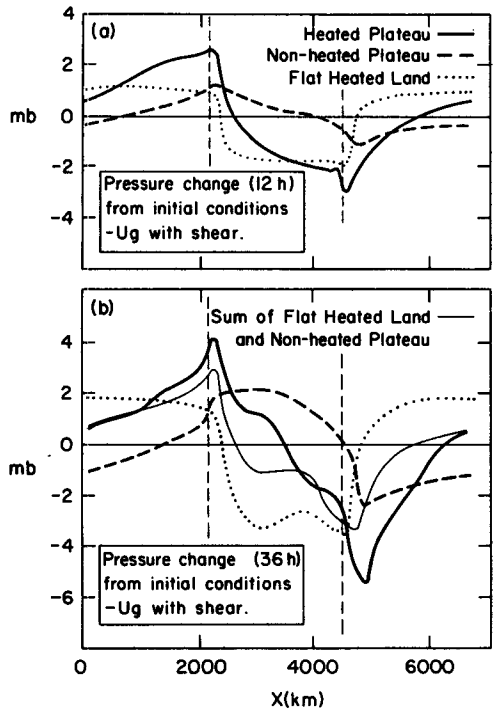

FIG. 2a. Horizontal profile of 12 h forecast surface pressure change from initial conditions for experiments A-1 (nonheated plateau), A-2 (heated plateau), and A-3 (flat heated land). Shear profile of u_g (profile A in Fig. 1) used in these experiments. The vertical dashed lines signify the edge of the top of the plateau.

FIG. 2b. As in Fig. 2a but for 36 h forecasts. The sum of surface pressure change from experiments A-1 and A-3 is also shown.

from the plateau case without surface fluxes (Experiment A-1, Fig. 2a) very closely resembles that determined from an analytic solution for flow over a similarly shaped plateau given by Queney (1948, Fig. 5). A trough about 1 mb deep has developed on the lee side and a ridge perturbation also of about 1 mb is shown on the windward side of the plateau. However, when strong surface heating over the plateau was allowed (Experiment A-2, Fig. 2a), the lee trough perturbation at 12 h intensified from just over 1 mb (without heating) to about 3 mb. Similar horizontal profiles of surface pressure change (within 0.3 mb of A-2 at 12 h at the ridge and trough) were produced in three variations of experiment A-2, with a 1000 km wide plateau, a 55 km grid length, and a more stable lower troposphere, respectively.

This result was similar to that of the 3-D experiments (BC) where an additional deepening of over 4 mb in 12 h was forecast for the SESAME I and IV lee troughs when surface fluxes were permitted. The cross-barrier wind component in these 3-D case simulations was stronger than in the 2-D experiments and probably accounts for the difference.

A third experiment (A-3) was performed with no elevated terrain but with the same land–ocean distribution used in Exp. A-2 to assess the degree to which the heat-low effect contributed to the intensification of the lee trough. A relatively uniform heat low over the continent developed by 12 h, similar to the difference pressure field from a pair of no-terrain 3-D experiments presented by BC (Fig. 25).

By 36 h (Fig. 2b), the lee trough from the heated experiment (A-2) increased to a perturbation over 5 mb deep. The symmetric windward- and leeside perturbations present in the nonheated plateau experiment (A-1) at 12 h were distorted by 36 h as a result of two effects. First, a column of air, which was potentially cooler than that in the initial field due to its history of ascent, was advected eastward across the plateau. Second, the coolness of this air over the plateau was also influenced by cold air advection from the north ($\partial\theta/\partial y \neq 0$ in experiments with shear) between the windward high and the lee trough. In a similar manner, the easterly advection of descended air enhanced by warm air advection from the south weakened the east–west pressure gradient on the east side of the lee trough. In actual cases over the south-central United States, this low-level warm air advection is limited by the sea surface temperature of the Gulf of Mexico and the residence time over heated land.

The development of the lee trough (or heat low) in various experiments with shear is portrayed in Fig. 3. As expected, the nonheated plateau case (Experiment 2D-1) showed no diurnal variation and reached a steady-state magnitude of 2 mb after 24 h. [For the mountain half-width (80 km) and mean wind speed (about 15 m s^{-1}) of this experiment, about 24–27 h of integration should be sufficient to produce a quasi-steady state mountain wave, according to Klemp and Lilly, 1978.] A second nonheated plateau experiment (A − 1A) with no bulk surface drag revealed that surface friction slightly intensifies the lee trough. This result is

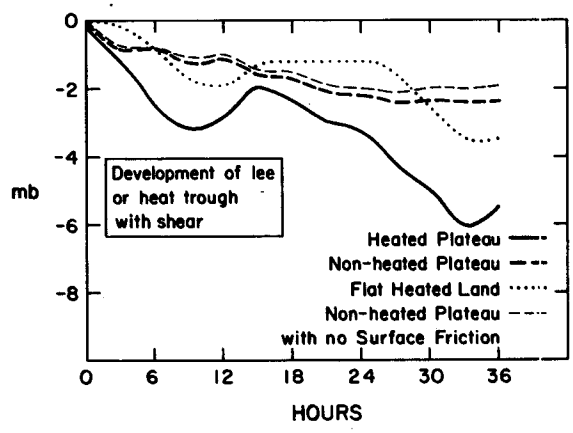

FIG. 3. Forecast development of lee or heat trough from experiments A-1 (nonheated plateau with surface friction), A-1A (nonheated plateau without surface friction), A-2 (heated plateau), and A-3 (flat heated land).

consistent with the findings of Buzzi and Tibaldi (1977) and Han et al. (1982). However, the surface frictional effect is quite small compared to that of the heating cycle.

The diurnal tendency of the flat land heat low (Exp. A-3) was similar to that of the heated plateau experiment (A-2) but the magnitude of the low was only 50–60% of that in Exp. A-2 (Fig. 3). If the intensification of the lee trough from surface heating were merely a superposition of the heat-low effect, the sum of the nonheated plateau and the heat-low curves in Fig. 2b would be approximately equal to that of the heated plateau. However, after taking this sum, 1–2 mb of the heated plateau perturbation in Fig. 2b remains unexplained. These 2-D simulations therefore suggest, as did the 3-D sensitivity tests in BC, that some additional effect or interaction between differential heating and the mountain wave must account for the additional deepening of the lee-side trough. The 3-D simulations in BC indicated that this additional effect was related to vertical mixing of momentum.

Cross sections of the height (h) change field were plotted to examine the changes in the pressure field above the surface. In the nonheated plateau experiment at 36 h (Fig. 4a), the windward ridge and lee trough perturbations both become weaker with height and both tilt upwind with height. When surface heating is allowed over the plateau (Fig. 4b), the lee trough becomes much more intense but it disappears quickly with height through the hot mixed layer, and a high pressure anomaly is present at the top of the mixed layer.

The surface pressure perturbations which developed with a constant u_g of 10 m s^{-1} (experiment series B) were much larger than those for the shear wind profile (experiment series A) (Figs. 5a, b). The trough perturbation in the heated plateau experiment (B-2), for instance, reached almost 6 mb at the end of day 1 (12 h) and over 13 mb by the end of day 2 (36 h). The stronger perturbations in this series of experiments are attributable to the stronger low-level geostrophic winds (through Bernoulli's theorem, e.g., Gill, 1982). Again, the addition of surface heating produced an extra intensification of both the lee trough and windward ridge.

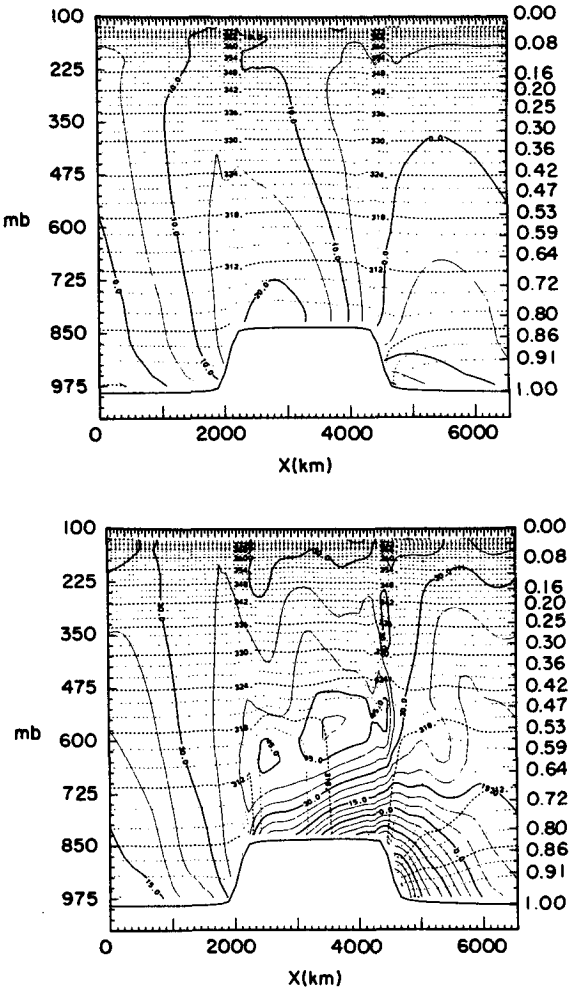

FIG. 4. Cross section of change in constant pressure surface heights (m) from initial conditions at 36 h for (a) experiment A-1 and (b) experiment A-2 (solid lines). Dotted lines are isentropes (K) at 36 h for experiment A-1.

b. *Effects on winds*

At 36 h, the wind and potential temperature fields from the nonheated plateau experiment with shear (A-1, Fig. 6) are at a virtual steady state. A well-defined downward extrusion of higher wind speeds is present above the lee slope, and the wind maximum axis slopes upwind with height. This structure resembles that simulated by Mahrer and Pielke (1975) for a flow over a ridge in a shearing environment. The upwind tilt is in agreement with simulations by Klemp and Lilly (1978) and Anthes and Warner (1978). A small perturbation in the potential temperature field exhibits approximately the same tilt.

In the heated plateau experiment (time sequence in Fig. 7a, b, c), momentum has been well-mixed through the daytime boundary layer, which is about 300 mb deep. During the daytime, winds are supergeostrophic in the lower part of the mixed layer and subgeostrophic in the upper part. An inertial oscillation in the mixed layer (half-period of 17.5 hours at 20°N, Blackadar, 1957) has reversed this pattern at 24 h (Fig. 7b) before the onset of mixing on day 2.

The leeside wind maximum at 12 h and 36 h appears to be located to the lee of the mixed layer rather than to the lee of the plateau. The maximum again slopes upwind with height, and is most concentrated at 12 h and 36 h when the boundary layer is deep and well-mixed. The intense acceleration which air parcels experience as they leave the mixed layer between 550

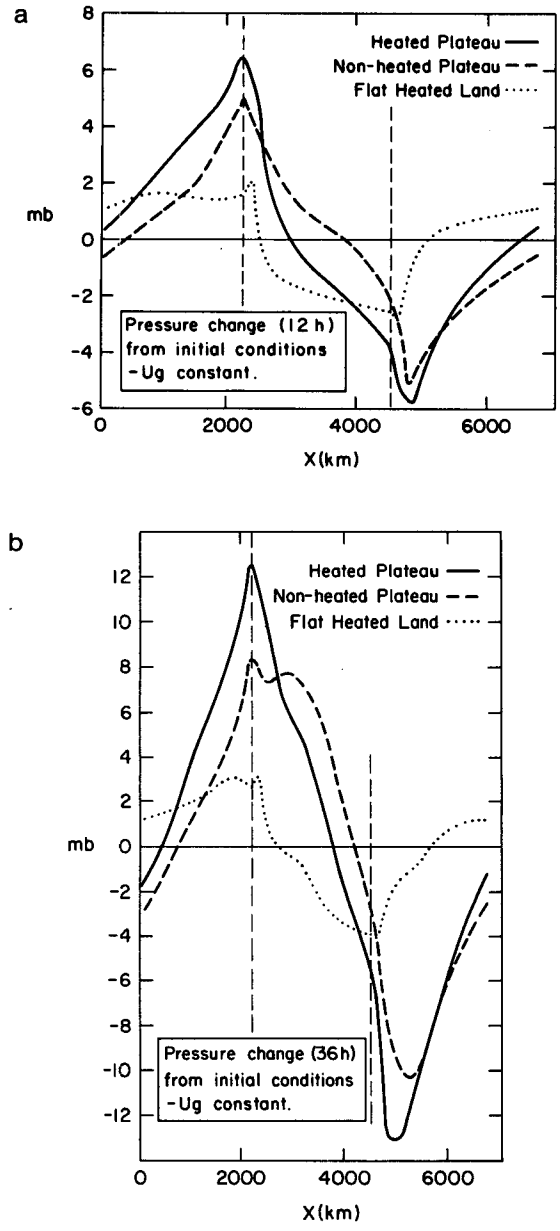

FIG. 5. As in Fig. 2 but for experiments with u_g = constant at 10 m s^{-1} (B-1, B-2, B-3); (a) 12 h, (b) 36 h.

and 675 mb and enter the wind maximum is supported by the strong pressure gradient in this same region shown in Fig. 4b. Convergence is apparent where the ambient westerly flow encounters slower moving air in the upper west end of the plateau mixed layer. These patterns suggest that deep vertical mixing of momentum over the plateau may extend the influence of the plateau upward and may be partly responsible for the enhancement of the lee trough and windward ridge when surface heating is present. This hypothesis is investigated in section 4c.

In the experiment in which the sea-level land area is heated (Exp. A-3), perturbations develop in the wind field which are similar to those from experiments with terrain. A wind maximum on the lee side of the deep, continental mixed layer and a minimum on the windward side both slope upwind with height. This pattern is most clearly defined at 18 h (Fig. 8a). After the surface heating during day 2 (36 h, Fig. 8b), the mixed layer is over 300 mb deep. A wind maximum is apparent to the lee of the mixed layer and convergence is present on the west side of the mixed layer, as they were in the heated plateau experiment (A-2). These features suggest that an isolated, deep boundary layer through which momentum is well-mixed may act as a permeable barrier to ambient flow even in the absence of terrain.

The increased intensity of the mountain wave which results from using a constant u_g of 10 m s^{-1} rather than the shear wind profile is also apparent in the wind perturbations. In the nonheated plateau experiment (B-1, Fig. 9), a wind maximum of over 20 m s^{-1} has developed by 36 h just above the top of the lee slope. A strong northerly component is present behind the lee trough. When surface heating is allowed over the plateau (Fig. 10), the lee wind maximum is about the same intensity, but it is again located, as with the shear wind profile (Fig. 7a, c), at the lee of the mixed layer between 500 and 600 mb rather than lower and nearer to the surface.

The southerly flow (low-level jet) of moist air ahead of the lee trough and the dryline are both important features of the severe storm environment which can be strongly influenced by the mountain wave. Benjamin and Carlson showed that the intensification of the

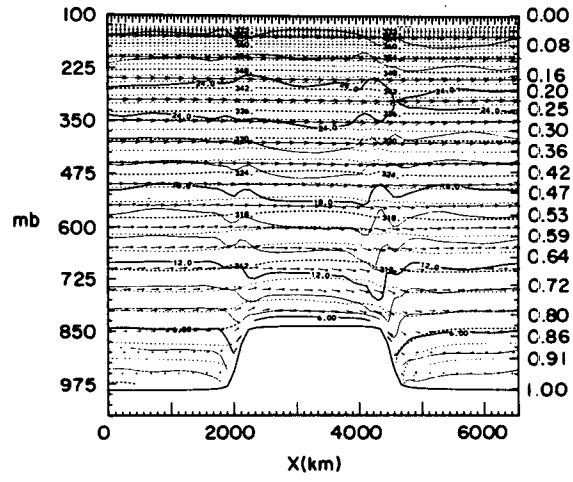

FIG. 6. 36 h forecast of horizontal wind and potential temperature from experiment A-1 (nonheated plateau, u_g with shear). Arrows denote (u, v) wind vector and length is proportional to magnitude. Solid lines are isotachs (m s^{-1}) of $(u^2 + v^2)^{1/2}$ and dotted lines are isentropes (K). Model terrain is denoted by solid line at bottom of figure.

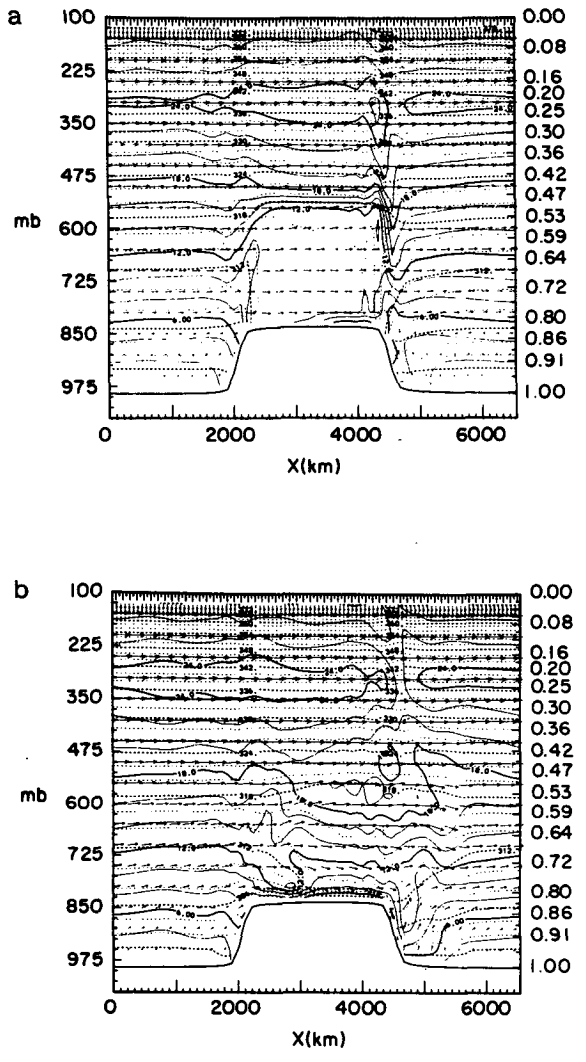

FIG. 7. As in Fig. 6 but for exp. A-2 (heated plateau). (a) 12 h forecast, (b) 24 h forecast, (c) 36 h forecast.

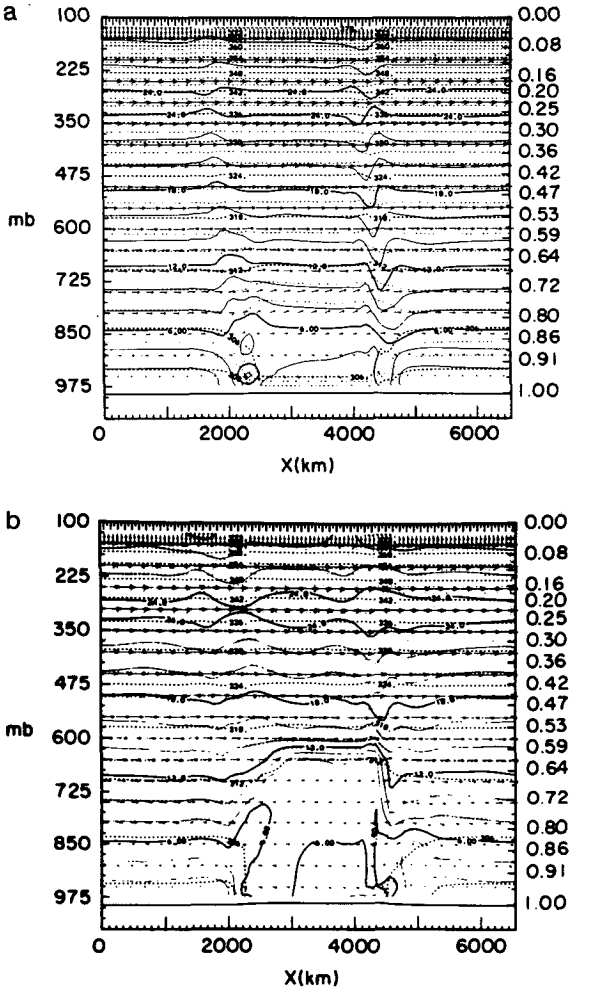

FIG. 8a. As in Fig. 6 but for exp. A-3 (flat heated land surrounded by ocean; surface index varies horizontally in same manner as in heated plateau experiments). (a) 18 h forecast, (b) 36 h forecast.

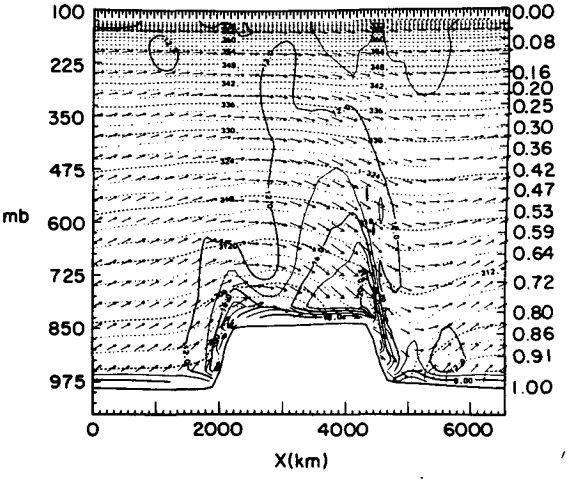

FIG. 9. As in Fig. 6 but h for experiment B-1 (nonheated plateau, u_g constant at 10 m s^{-1}), 36 h forecast.

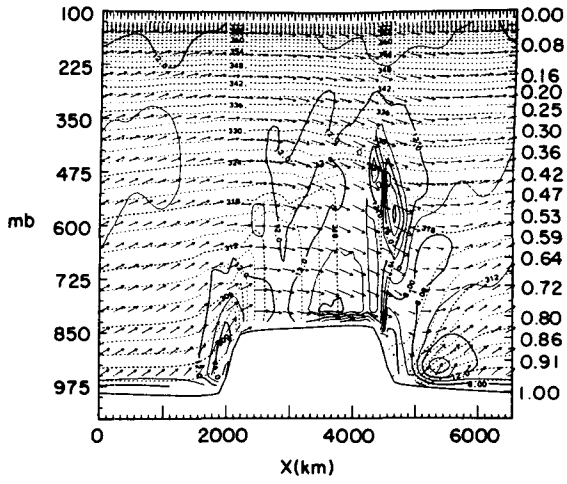

FIG. 10. As in Fig. 6 but for experiment B-2 (heated plateau), 36 h forecast.

lee trough associated with surface heating also forced an increase southeasterly low-level flow off the Gulf of Mexico. This flow appeared to retard eastward propagation of the dryline during the day and force its retrogression during the early evening hours. In the 2-D experiments of this paper, a similar diurnal variation occurred in the southerly flow ahead of the lee trough. Figure 11 depicts the temporal variation of winds east of the lee trough in heated plateau experiments with both wind profiles. The afternoon deepening of the lee trough forced a strongly ageostrophic, isallobaric component in both experiments. The easterly component disappeared after sundown (12 h) as an inertial oscillation developed. Little change occurred after 18 h (midnight local time) until redeepening of the lee trough on day 2 again decreased the u component. The diurnal variation of the ageostrophic u component in the low-level jet favors strongest destabilization by differential advection in the late afternoon and early evening hours, as suggested in section 4c of BC.

It may also be noted in Figs. 7a–c that the thermal gradient accompanying the upward sloping elevated mixed layer dictates that the southerly low-level flow must decrease with height. This configuration by which a northerly thermal wind, produced by confluence between a warm continental airstream and a cooler airstream to its east, favors a southerly low-level jet was also noted by Means (1954).

c. *Effects of differential vertical mixing of momentum*

About half of the additional lee troughing (over 4 mb in 12 h) resulting from allowing surface heat fluxes in SESAME I case simulations performed by BC was linked to changes in vertical mixing of momentum. This was determined by comparing two 12 h simulations, both with surface heating but with no vertical mixing of momentum allowed in one of the experiments. However, even though identical initial conditions and surface characteristics were used, it was possible for heat flux (and hence, differential heating) to vary between these experiments since the heat flux is itself a function of momentum mixing (through the friction velocity, u^*; Zhang and Anthes, 1982, Eq. 11). Thus, the difference in the lee trough between these 3-D experiments still could have been partially attributed to a difference in the heat-low effect caused by differential heating between the dry Mexican plateau and the Gulf of Mexico.

A similar but more carefully controlled series of 2-D tests were devised to isolate mountain wave sensitivity to vertical mixing of momentum. In the additional experiments using different wind profiles with and without terrain (A-4, A-5, B-4, B-5), vertical mixing of momentum was set equal to zero in the free convection regime but mixing of heat was still allowed. (Mixing in other regimes was negligible.) At the same time, the heat flux from the surface layer and the surface layer temperature (H_0 and θ_a, respectively; see Zhang and Anthes, 1982) were specified to be identical in space and time to those from corresponding experiments with mixing of momentum (A-2, A-3, B-2, B-3). This procedure constrained the heating of the mixed layer and the heat-low effect in experiments without mixing of momentum to be equal to those in the experiments with mixing of momentum. Accordingly, the thermal structure appears very similar in these experiments.

The horizontal wind and potential temperature cross section from one of these additional experiments (A-4) is presented as Fig. 12. In this heated plateau ex-

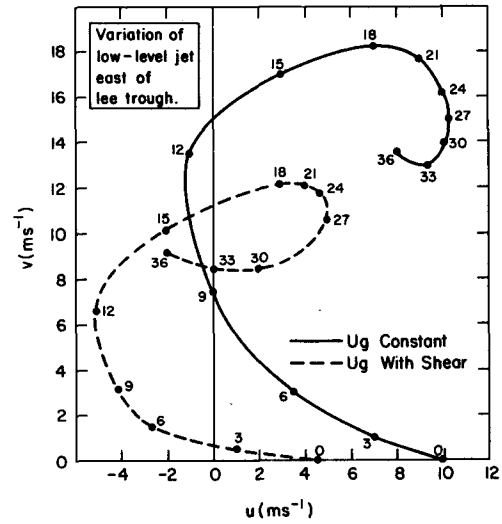

FIG. 11. Temporal variation of low-level jet east of lee trough. Hodograph shows wind from 0–36 h at point east of the lee trough with the strongest v component. The location of this point is at σ = 0.96 and moves eastward from the slope of the plateau at t = 0 to 200 km east of the plateau slope by t = 36 h. In the experiment with shear, u_g at this point varies from 4.0 to 1.2 m s^{-1}.

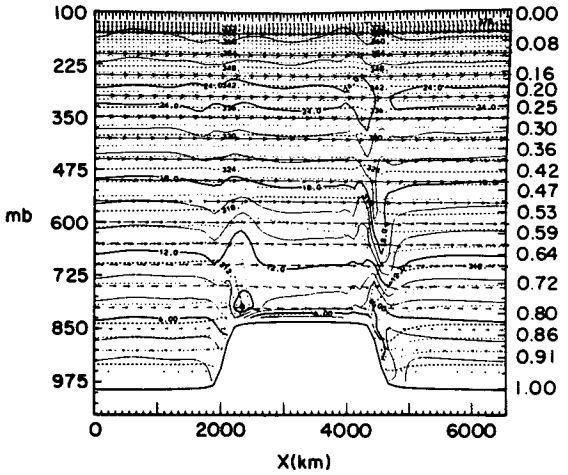

FIG. 12. As in Fig. 6 but for experiment A-4 in which no vertical mixing of momentum was allowed. Surface heat flux and potential temperature were specified to be equal to those from experiment A-2 (Fig. 7) in which vertical mixing of momentum was included.

periment without vertical mixing of momentum, the divergence to the lee of the mixed layer is noticeably smaller (e.g., wind magnitude increasing from 14 to 19 m s^{-1} at 600 mb) than it was in the corresponding experiment with mixing of momentum (10 to 18 m s^{-1} at 600 mb).

To isolate the effects of mixing of momentum on the pressure distribution, the perturbations in surface pressure and heights from experiments without mixing of momentum were subtracted from those with mixing. These pressure differences (Fig. 13a, b—surface pressure) may be interpreted as the effects of differential mixing of momentum, including secondary feedback effects such as changes in vertical motion or horizontal temperature advection.

In all cases, differential mixing tended to produce a windward ridge and lee trough regardless of whether or not elevated terrain was present. However, in a shearing environment, the presence of the plateau enabled the mixed layer to entrain air with higher momentum and enhance the horizontal gradient of momentum mixing. In an environment with constant geostrophic wind, on the other hand, the presence of the plateau did not appreciably change the differential mixing of momentum effect. It also appears that this effect is not dependent upon the presence of geostrophic shear so much as on the presence of moderately strong lower tropospheric winds. The existence of mixing assures stronger flow in the shallow surface layer and that a horizontal gradient of surface stress occurs between regions with and without mixing regardless of the ambient shear. Although it is not demonstrated here, there may also be an effect of vertical mixing in the presence of uniform surface heating along sloping terrain when a horizontally constant vertical wind shear is present since the top of the mixed layer over higher terrain will entrain higher momentum than that over lower terrain.

The structure of horizontal winds from these 2-D experiments with surface heating suggests two mechanisms through which differential vertical mixing of momentum could enhance the intensity of a leeside surface pressure trough. First, the mass divergence which produces lee trough development in a two-dimensional model is associated with positive values of $(\partial u/\partial x)_z$ upstream of the jet typically found near the lee side. This divergence can be concentrated by an environment in which strong vertical mixing of momentum takes place over the plateau or mountain but decreases or becomes nonexistent over the lower terrain, as shown in the schematic in Fig. 14. The mixing decreases winds in the upper part of the mixed layer (in a shearing environment) and also decreases the mean wind through the mixed layer through increased surface stress. (The mean wind below $\sigma = 0.529$ at a point in the middle of the plateau changed less than 0.04% in 12 hours in Exp. A-4 without momentum mixing, but decreased 12% in Exp. A-2 in which momentum mixing was allowed.) If the maximum in u component downstream remains large due to propagation of gravity waves from the forcing of flow over the barrier, the increased value of $\partial u/\partial x$ (divergence) will enhance the intensity of the surface lee trough. This assumes that the extra mass divergence to the lee of the upper part of the mixed layer is not compensated by mass convergence elsewhere in the column.

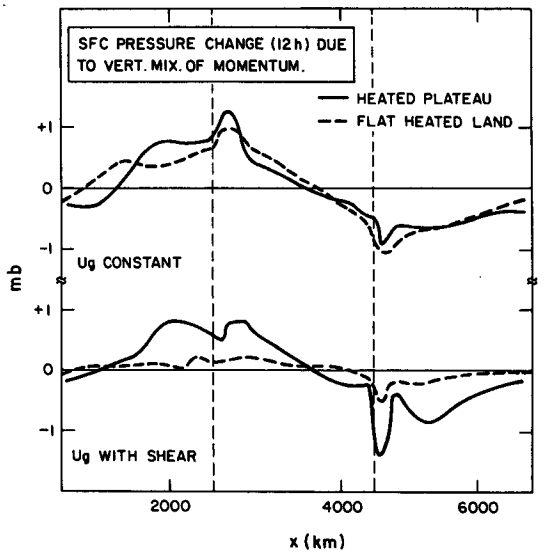

FIG. 13. Horizontal profile of surface pressure change at 12 h due to vertical mixing of momentum. Perturbations are determined by subtracting change in experiment without mixing of momentum from change in experiment with mixing of momentum. (a) u_g constant at 10 m s^{-1}; heated plateau (Exp. B-2 minus Exp. B-4) and flat heated land (Exp. B-3 minus Exp. B-5). (b) u_g with shear; heated plateau (Exp. A-2 minus Exp. A-4) and flat heated land (Exp. A-3 minus Exp. A-5).

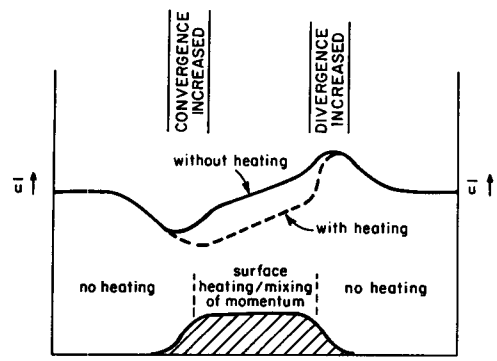

FIG. 14. Schematic showing effect of vertical mixing of momentum over dry plateau on mountain wave pressure perturbations. Shape of the u (cross-barrier) component for inviscid flow across a plateau (solid line) is from Queney (1948). The dashed line indicates the perturbation produced in the upper part of the mixed layer by surface heating over the plateau.

The second hypothesis is as follows. Since mixing of momentum increases low-level wind speeds, warm-air advection near the edge of the plateau is also increased, especially at the base of the mixed layer where the greatest warming has occurred. An examination of the height change perturbations produced by vertical mixing of momentum (not shown) indicated that 50–80% of the surface pressure perturbations in Fig. 13 was also present near the top of the mixed layer. The heated plateau experiment with shear in which the greatest mixing of momentum occurred among this set of experiments, showed the largest contribution (50%) to the surface pressure perturbation from near the base of the mixed layer. These results suggest that the first hypothesized mechanism is dominant in producing the differential mixing effect, but that the second may also be significant.

It is also possible that the small changes in stability produced by mixing of momentum significantly altered the environment for mountain wave development. While all of these possible effects are interrelated to the extent that they cannot be easily isolated, it is clear that the changes are all due to mixing of momentum.

The variation of soil moisture between the dry Mexican plateau and the moist coastal plain and Gulf of Mexico imposes a gradient of boundary layer depth and, therefore, vertical mixing of momentum in the region where the enhanced lee troughing occurs. Thus, the increase of lee troughing and windward side ridging (a similar soil moisture gradient exists on the west coast of Mexico) which resulted when surface heating was allowed in 3-D simulations by BC, are both consistent with the hypothesized differential mixing mechanism.

It is cautioned that the results showing this effect may be dependent upon the particular boundary-layer model used. Mahrt (1976) has pointed out that significant vertical gradients of moisture may exist in the well-mixed boundary layer. Similarly, Lenschow et al. (1980) have reported that wind shear may exist in a well-mixed layer which is comparable in magnitude to the geostrophic shear. Since the version of the multilevel boundary-layer model used in these experiments tends to completely mix absolute moisture and momentum, the importance of the differential mixing mechanism may be smaller than indicated by these 2-D experiments.

d. Development of the elevated mixed layer

The idealized conditions of the 2-D experiments permit a clear perspective on the behavior of the mixed layer as it convectively decouples from the surface near the edge of the plateau. The advection of this layer over the ocean (low elevation region without surface heating) is depicted in Fig. 7c. At 36 h, the elevated mixed layer may be recognized as the layer generally between 550 and 800 mb near the east end of the domain where isentropes are more widely spaced and are strongly tilted toward the vertical. The east–west temperature gradient within the mixed layer reflects the gradient in residence time over the heated plateau.

A region of low-level convergence accompanies the separation of the mixed layer from the surface. Westerly momentum is mixed downward over the heated plateau creating a zone near the surface with an ageostrophic west wind of greater than 4 m s^{-1}. However, east of the plateau, a strong ageostrophic easterly component (Fig. 11) has developed which is an isallobaric inflow toward the lee trough.

A sloping frontal zone is formed as the mixed layer overruns the potentially cooler air to its east. The differential advection which increases stability at the base of this layer is apparent east of the plateau in Fig. 7a–c. A continuity chart of the leading edge of the elevated mixed layer [identified as the 2 K (100 mb)$^{-1}$ isopleth, indicating near-neutral stability] is provided in Fig. 15. In Fig. 15a (from the heated plateau experiment, A-2), the lower part of the mixed layer advances most rapidly during the first 12 h. This behavior occurs since low levels are heated earlier in the day before the boundary layer builds to its eventual maximum height and since winds (ventilation) are constant with height at this time due to mixing. During the night however, the upper part of the mixed layer catches up to the lower portion, due to the inertial oscillation which produces supergeostrophic velocities in that volume (Fig. 7b). Some vertical compression of the mixed layer appears to take place, particularly at lower levels where it is forced up over a wedge of potentially cooler air to the east.

This compression was even more apparent in a continuity chart (Fig. 15b) of the elevated mixed layer from the flat land–ocean case (Exp. A-3). Again, the base of the heated layer forms a sloping frontal zone. The advection of the mixed layer reached a maximum late at night, as in the heated plateau experiment, as a result of the inertial oscillation in the mixed layer. This be-

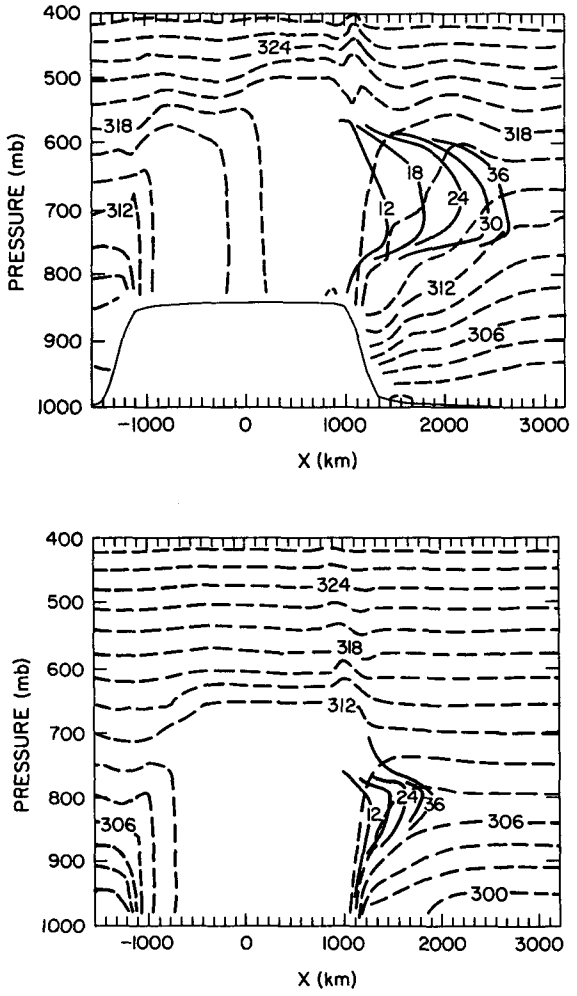

FIG. 15. Continuity chart of elevated mixed layer for (a) Exp. A-2 (heated plateau) and (b) Exp. A-3 (flat heated land). Solid lines are position of 2 K (100 mb)$^{-1}$ stability isopleth near leading edge of elevated mixed layer as it is advected downstream. Hours from initial time are noted at edge position. Dotted lines are isentropes (K) at 36 h.

havior suggests that the stabilizing effect from differential advection downwind of the plateau is retarded during the afternoon hours and becomes strongest at night.

The variation of soil moisture appeared to be crucial in the production of elevated mixed layer restraining inversions. When strong surface heating was allowed at low elevations as well as over the plateau (Exp. A-8, not shown), the vertical gradient of potential temperature was almost nonexistent.

Two major effects of the elevation of the heat source are apparent in a comparison of Figs. 15a and 15b. First, the potential temperature of the plateau mixed layer is somewhat higher ($\theta \sim 318$ K) than that of the sea-level mixed layer ($\theta \sim 311$ K). This difference is related to the typical lower tropospheric stability incorporated in the initial sounding. Second, the ventilation of the high-level heat source is stronger in an environment of vertical wind shear. These cause the elevated mixed layer to be more impressive in the heated plateau case, being deeper and possessing somewhat higher temperatures which produce larger stability at its base.

5. Discussion and conclusions

A variety of 2-D experiments have been performed which demonstrate that differential heating between a dry plateau and moist lowlands produces a daytime intensification of the leeside surface pressure trough which occurs in the presence of flow across the plateau. This same configuration of flow across a dry elevated heat source toward lower, moist regions also consistently produced a low-level stable layer downstream of the heated region. This inversion was formed as the hot mixed layer originating over the plateau overran potentially cooler air downstream. In a companion paper, Benjamin and Carlson (1986) found that both of these effects occurred in 3-D regional-scale simulations of severe storm cases and suggested that in certain cases, they may act to delimit the region and time interval in which convective storm outbreaks are most likely.

In this study, a 2-D model with a multilayer boundary-layer parameterization was used to study the effects of surface heating on flow over a 2000 km wide plateau. When no surface heating was allowed, fields of the surface pressure, wind and potential temperature were found to closely resemble those from other mountain wave simulations. When differential heating was allowed, the magnitude of the surface lee trough increased by 2–4 mb. This increase was largest in the late afternoon and early evening hours. This variation, in turn, forced a diurnal modulation of the low-level flow ahead of the lee trough, which is often the major source of moisture in outbreaks of convective storms in the south-central United States and some other regions of the world, such as China and Argentina.

The diurnal variation of the lee trough in the presence of differential heating was determined to be primarily a product of two mechanisms, both related to surface heating. The first is a heat-low effect by which a high pressure perturbation developed at and above the top of the heated mixed layer, causing divergence aloft and a decrease of surface pressure over the heated region. This effect may also occur in the absence of elevated terrain as well as in the absence of ambient flow. The advection of air with a history of ascent or descent and north–south temperature advection in the experiments of this study tended to distort the horizontal uniformity of the heat low as the integration time increased beyond 12 h. The heat-low effect appeared to be responsible for the majority of the difference between plateau pressure perturbations with and without surface heating.

A second effect which enhanced mountain-wave surface pressure perturbations in the presence of differential heating was the horizontal variation of vertical mixing of momentum. A comparison of carefully controlled 2-D experiments with and without mixing of momentum revealed that a mountain-wavelike perturbation of about 1 mb on the windward and lee sides of the deep mixed layer could be attributed solely to this mechanism. Since the heat low contributed about 2 mb to the entire perturbation, it is estimated that the differential mixing process may be responsible for roughly 30% of the enhancement of the lee trough from surface heating in cases such as those simulated here. This result is consistent with the estimate of 50% determined by Benjamin and Carlson (1984) in 3-D experiments, since the latter was exaggerated by an imperfect control upon surface heating.

Significantly, this perturbation appeared even in experiments in which elevated terrain was absent. The plateau enhanced this effect most sharply in the presence of vertical wind shear, since it enabled the mixed layer to entrain higher momentum at its top and subsequently transfer it to the surface layer. But even without the plateau, isolated deep mixed layers produced surface pressure perturbations which appeared to result from a blocking effect. Stern and Malkus (1953) analytically determined that the larger-scale perturbation from flow over a heated island was identical to that produced by an "equivalent mountain" of a certain shape. However, their formulation accounted only for eddy diffusivity of heat and not for that of momentum.

The 2-D experiments also helped to clarify the environmental features most important to the formation of elevated mixed layer restraining inversions or "lids." Other than differential advection or vertical wind shear, the most important contributor to this type of lid formation was an upstream gradient of soil moisture. An elevated mixed layer was formed even without the plateau if differential heating was present, but none was formed in a plateau experiment with uniform heating. Second, the downstream decrease in elevation enhanced the strength of the inversion because of the higher potential temperature which developed in the plateau mixed layer. Last, the 3-D experiments of BC also indicated that stratus clouds over moist lowlands could further enhance the differential heating and thereby, the "lid" effect.

Since the necessary conditions of soil dryness over the plateau of Mexico and the southwest United States and ambient westerly flow are both met primarily in the late winter and spring, the diurnal variation of the lee trough and southerly flow ahead of it as well as the elevated mixed layer lid may be expected most commonly at that time of year. Accordingly, it is suggested that year-to-year variations in their role in the downstream development of severe storm environments may be related to late-winter and spring anomalies of precipitation over the plateau and adjacent lowlands.

Acknowledgments. I wish to express my gratitude to Professor Toby Carlson for his guidance while this research was begun as part of my dissertation work at The Pennsylvania State University and for a constructive review of a recent draft. I also thank John M. Brown, Ron Alberty, and Joseph Klemp for helpful discussions and suggestions regarding the paper, and Hope Hamilton and Janell Petersen for preparing the manuscript. This study was supported in part under U.S. Air Force Grants AFOSR-79-0125 and AFOSR-83-0064.

REFERENCES

Alaka, M. A., Ed., 1960: The airflow over mountains. World Meteor. Organization, Tech. Note No. 34, 135 pp.

Anthes, R. A., and T. T. Warner, 1978: The development of mesoscale models suitable for air pollution and other mesometeorological studies. *Mon. Wea. Rev.*, **106,** 1045–1078.

——, and D. Keyser, 1979: Tests of a fine-mesh model over Europe and the United States. *Mon. Wea. Rev.*, **107,** 963–984.

——, Y.-H. Kuo, S. G. Benjamin and Y.-F. Li, 1982: The evolution of the mesoscale environment of severe local storms: Preliminary modeling results. *Mon. Wea. Rev.*, **110,** 1187–1213.

Barry, R. G., 1981: *Mountain Weather and Climate,* Methuen, 313 pp.

Benjamin, S. G., and T. N. Carlson, 1986: Some effects of surface heating and topography on the regional severe storm environment. Part I: Three-Dimensional simulations. *Mon. Wea. Rev.*, **114,** 307–329.

Blackadar, A. K., 1957: Boundary-layer wind maxima and their significance for the growth of nocturnal inversions. *Bull. Amer. Meteor. Soc.*, **38,** 283–290.

Bleck, R., 1977: Numerical simulation of lee cyclogenesis in the Gulf of Genoa. *Mon. Wea. Rev.*, **105,** 428–445.

Bleeker, W., and Andre, M. J., 1951: On the diurnal variation of precipitation, particularly over central U.S.A., and its relationship to large-scale orographic circulation systems. *Quart. J. Roy. Meteor. Soc.*, **77,** 260–271.

Buzzi, A., and S. Tibaldi, 1977: Inertial and frictional effects on rotating and stratified flow over topography. *Quart. J. Roy. Meteor. Soc.*, **103,** 135–150.

Carlson, T. N., and F. H. Ludlam, 1968: Conditions for the occurrence of severe local storms. *Tellus,* **20,** 203–226.

——, R. A. Anthes, M. Schwartz, S. G. Benjamin and D. G. Baldwin, 1980: Analysis and prediction of severe storms environment. *Bull. Amer. Meteor. Soc.*, **61,** 1018–1032.

——, S. G. Benjamin, G. S. Forbes and Y.-F. Li, 1983: Elevated mixed layers in the regional severe storm environment: Conceptual model and case studies. *Mon. Wea. Rev.*, **111,** 1453–1473.

Egger, J., 1974: Numerical experiments on lee cyclogenesis. *Mon. Wea. Rev.*, **102,** 847–860.

Gao, Y.-X., M.-C. Tang, S.-W. Luo, Z.-B. Shen and C. Li, 1981: Some aspects of recent research on the Qinghai-Xizang Plateau meteorology. *Bull. Amer. Meteor. Soc.*, **62,** 31–35.

Gill, A. E., 1982: *Atmosphere-Ocean Dynamics,* Academic Press, 662 pp.

Han, Y. J., K. Ueyoshi and J. W. Deardorff, 1982: Numerical study of terrain-induced mesoscale motions in a mixed layer. *J. Atmos. Sci.*, **39,** 2464–2476.

Holton, J. R., 1967: The diurnal boundary layer wind oscillation above sloping terrain. *Tellus,* **19,** 199–205.

Klemp, J. B., and D. K. Lilly, 1975: The dynamics of wave-induced downslope winds. *J. Atmos. Sci.*, **32,** 320–339.

Klemp, J. B., and D. K. Lilly, 1978: Numerical simulation of hydrostatic mountain waves. *J. Atmos. Sci.*, **35,** 78–107.

Lenschow, D. H., J. C. Wyngaard and W. T. Pennell, 1980: Mean-field and second-moment budgets in a baroclinic, convective boundary layer. *J. Atmos. Sci.*, **37,** 1313–1326.

Lettau, H. H., and K. Lettau, Eds., 1978: Exploring the world's driest climate. Rep. 101, Inst. Environ. Studies, University of Wisconsin, Madison, 264 pp.

Mahrer, Y., and R. A. Pielke, 1975: A numerical study of the airflow over mountains using the two-dimensional version of the University of Virginia mesoscale model. *J. Atmos. Sci.*, **32,** 2144–2155.

Mahrt, L. 1976: Mixed layer moisture structure. *Mon. Wea. Rev.*, **104,** 1403–1407.

Means, L. L., 1954: A study of the mean southerly wind maxima in low levels associated with a period of summer precipitation in the middle west. *Bull. Amer. Meteor. Soc.*, **35,** 166–170.

Mosiño Aleman, P. A., and E. Garcia: The climate of Mexico. *World Survey of Climatology,* 11. *Climates of North America,* R. A. Bryson and E. F. Hare, Eds., Elsevier Scientific, 345–404.

Ookouchi, Y., M. Segal, R. C. Kessler and R. A. Pielke, 1984: Evaluation of soil moisture effects on the generation and modification of mesoscale circulations. *Mon. Wea. Rev.*, **112,** 2281–2292.

Queney, P., 1948: The problem of airflow over mountains: A summary of theoretical studies. *Bull. Amer. Meteor. Soc.*, **29,** 16–26.

Raymond, D. J., 1972: Calculation of airflow over an arbitrary ridge including diabatic heating and cooling. *J. Atmos. Sci.*, **29,** 837–843.

Reiter, E. R., and M. Tang, 1984: Plateau effects on diurnal circulation patterns. *Mon. Wea. Rev.*, **112,** 638–651.

Smith, R. B., 1979: The influence of mountains on the atmosphere. *Advances in Geophysics,* Academic Press, **21,** 87–230.

Stern, M. E., and J. S. Malkus, 1953: The flow of a stable atmosphere over a heated island, Part II. *J. Meteor.*, **10,** 105–120.

Tang, M., and E. R. Reiter, 1984: Plateau monsoons of the Northern Hemisphere: A comparison between North America and Tibet. *Mon. Wea. Rev.*, **112,** 617–637.

Tibaldi, S., A. Buzzi and P. Malguzzi, 1980: Orographically induced cyclogenesis: Analysis of numerical experiments. *Mon. Wea. Rev.*, **108,** 1302–1314.

Zhang, D., and R. A. Anthes, 1982: A high-resolution model of the planetary boundary layer—Sensitivity tests and comparisons with SESAME-79 data. *J. Appl. Meteor.*, **21,** 1594–1609.